World Academy of Science, Engineering and Technology
International Journal of Electronics and Communication Engineering
Vol:3, No:5, 2009

Negative Slope Ramp Carrier Control for High Power Factor Boost Converters in CCM Operation

T. Tanitteerapan E.Thanpo

***Abstract*—**This paper, a simple continuous conduction mode (CCM) pulse-width-modulated (PWM) controller for high power factor boost converters is introduced. The duty ratios were obtained by the comparison of a sensed signal from inductor current or switch current and a negative slope ramp carrier waveform in each switching period. Due to the proposed control requires only the inductor current or switch current sensor and the output voltage sensor, its circuit implementation was very simple. To verify the proposed control, the circuit experimentation of a 350 W boost converter with the proposed control was applied. From the results, the input current waveform was shaped to be closely sinusoidal, implying high power factor and low harmonics.

***Keywords*—**High power factor converters, boost converters, low harmonic rectifiers, power factor correction, and current control.

I. Introduction

BOOST converter is one of the most popular choices for using as the high power factor converter. The converter is supplied from a full wave rectified line voltage and operated so that the input current follows the input voltage. The input current waveshaping can be achieved by using a number of techniques. When the converter is operated at fixed frequency and fixed duty ratio in the discontinuous conduction mode (DCM), the low frequency component of the input current is approximately proportional to the input voltage, so that the power is automatically close to unity [1]. However, the DCM operation causes a large current stress on semiconductors and demands more effort to attenuate the current ripple so as to have a satisfactory low electromagnetic interference (EMI) to the line. Therefore, in medium and high power applications, the continuous conduction mode (CCM) is preferred because the current stress and current ripple become too large when operating the converter in the DCM. Traditionally, to operate the boost converter as high power factor converter in the CCM, the conventional control as shown in Fig.1 [2] is applied. A sensed inductor current signal $R_s i_g(t)$ is compared with the current loop reference signal $v_q(t)$ at the current feedback loop $A_i(s)$. The current loop signal $v_q(t)$ is generated by multiplying the sensed full wave rectified input line voltage $v_g(t)$ and the control signal V_m from the error amplifier in the voltage feedback loop $A_v(s)$ at the multiplier. The amplified error signal $v_i(t)$ from the current feedback loop $A_i(s)$ is compared with the fixed frequency triangle waveform $v_c(t)$ at the comparator for pulse width modulator, adjusting the power switch duty ratio so as to minimize the error between the reference signal $v_q(t)$and the sensed inductor current signal $R_s i_g(t)$ resulting the input current waveform $i_g(t)$ is shaped to be proportional to the full wave rectified line voltage $v_g(t)$. The output voltage V_o is controlled by varying the scale factor between the rectified line voltage $v_g(t)$ and the current reference $v_q(t)$ from the multiplier output. So, because the conventional control requires many devices (the input sensor, the output voltage sensor, the inductor current sensor, the multiplier, the error amplifier in the voltage feedback loop $A_v(s)$, the error amplifier in the current feedback loop $A_i(s)$), then, its control circuit implementation is very complex.

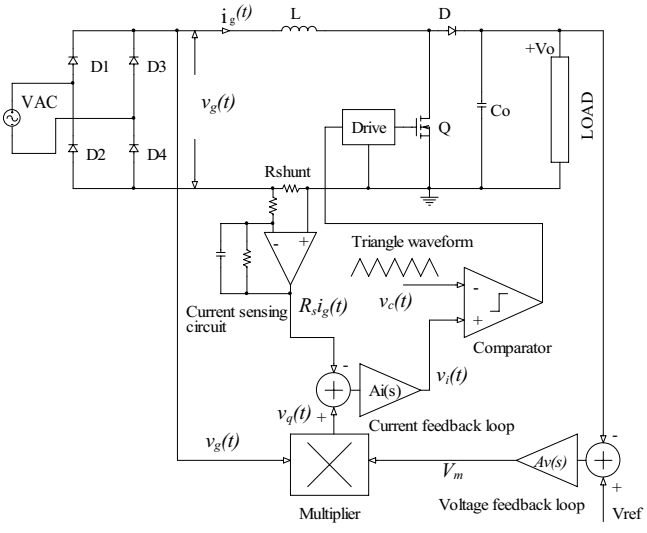

Fig. 1 Boost PFC converter with conventional controller

A number of papers [3]-[13] have been dedicated to simplify the complexity of conventional control circuit implementation in [2]. These papers eliminated the multiplier, the input

T. Tanitteerapan is with Power Electronics and Circuit Systems in Department of Electrical Technology Education, Faculty of Industrial Education, King Mongkut's University of Technology Thonburi, 126 Prachauthit, Bangmod, Tungkru, 10140 Thailand (corresponding author to provide phone: 662-470-8540; fax: 662-427-8541; e-mail: tanes_kmutt@yahoo.com).

E. Thanpo is with Electrical Power Department, Lopburi Technical Collage, Narai Maharaja, Thahin, Lopburi Province, Thailand.

voltage sensor, and the error amplifier in the current feedback loop $A_i(s)$ in the control circuit. Some method fulfilled that purpose under the penalty of higher current distortion [3]. The nonlinear-carrier (NLC) control proposed in [4] and [5] is one of good example for the simple CCM operation control technique. The sinusoidal switch current is sensed to compare with the nonlinear carrier waveform in each switching period for achieve the sinusoidal input current waveshape or high power factor condition. The input line voltage sensor, the multiplier, and the error amplifier in the current feedback loop $A_i(s)$ as shown in the conventional control technique in Fig.1 are not required in the NLC controller.

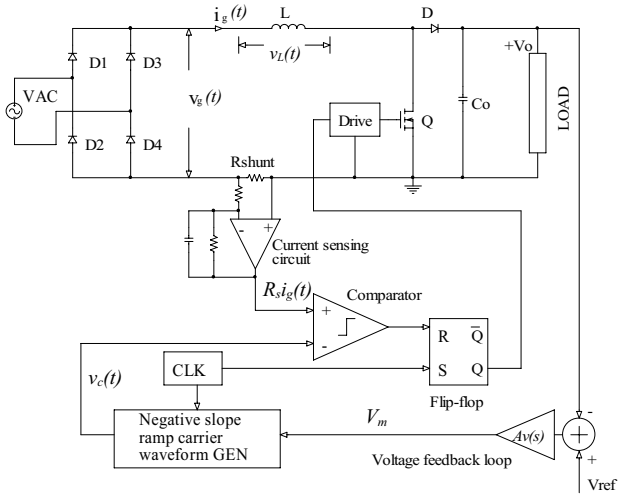

(a)

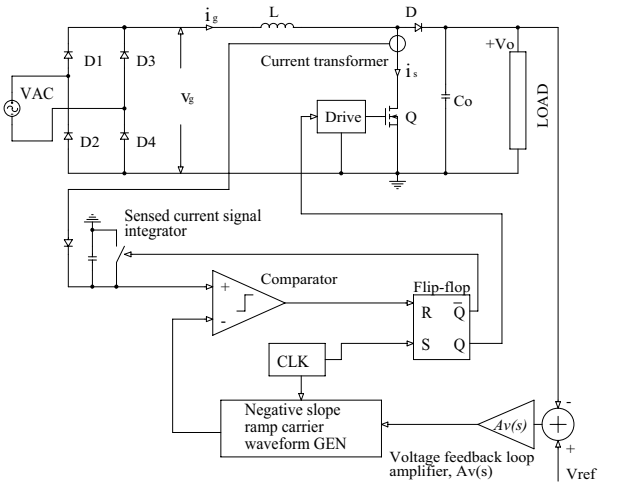

(b)

Fig. 2 High power factor boost converter with proposed controller: (a) inductor current sensing type and (b) switch current sensing type

The purpose of this paper is to present a simple PWM controller in the CCM operation for the high power factor boost converter as shown in Fig.2a and b. The proposed controller uses the basic principle like as the principle used in the NLC controller in [4] and [5] that the duty ratios are obtained by the comparison of the sensed current and the parabolic carrier waveform in each switching period. The proposed controller obtains the duty ratio in each switching period from the comparison of the negative ramp carrier waveform $v_c(t)$ and the sensed inductor current signal as shown in Fig2a and sensed switch current signal as shown in Fig 2b. So, the input voltage sensor, the error amplifier in the current feedback loop $A_i(s)$, and the multiplier as used in the conventional control technique are not required.

The design considerations of proposed controller are detailed in section II, and finally, the circuit experiment of 350W high power factor boost converter with proposed control is discussed in section IV.

II. Design Consideration for Proposed Control

The high power factor boost converter shown in Fig.1 and 2 is well-known switched-mode converter that is capable of producing a dc output voltage greater than the input voltage. Considering in one switching period when switch Q is turned on, the inductor is connected to ground, the inductor voltage $v_L(t)$ for this subinterval is given by

$$v_L(t) = V_g \tag{1}$$

where V_g is the input voltage.
When the switch Q is turned off, the inductor is connected to the output, the inductor voltage $v_L(t)$ is then

$$v_L(t) = V_g - V_o \tag{2}$$

where V_o is the output voltage.
Equations (1) and (2) are used to sketch the inductor voltage waveform shown in Fig.3.

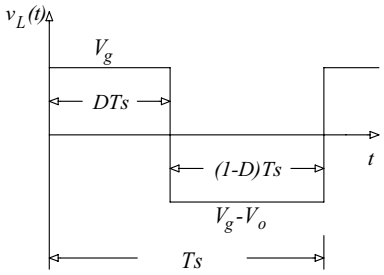

Fig. 3 Inductor voltage $v_L(t)$ waveform of boost converter in CCM operation

The figure shows that the average value in one switching period of the inductor voltage waveform is equal to zero so that

$$\langle v_L(t)\rangle_{T_s} = \frac{1}{T_s}\int_0^{T_s} v_L(t)dt = V_g D - (V_g - V_o)(1-D) = 0 \quad (3)$$

where $\langle v_L(t)\rangle_{T_s}$ is the average value of the inductor voltage $v_L(t)$ in one switching period, T_s is the switching time period, and D is the duty ratio.
From equation (3), the input voltage V_g can be given by

$$V_g = V_o(1-D) \quad (4)$$

In the high power factor converter operation, the input voltage V_g, the output voltage V_o and the duty ratio D are varied with time. So, the relation depending on time of equation (4) can be written as

$$v_g(t) = v_o(t)(1-d(t)) \quad (5)$$

where $v_g(t)$ is the input voltage, $d(t)$ is the duty ratio and $v_o(t)$ is the output voltage.
When the unity power factor condition occurs, the converter looks like a resistor, which is called as the emulated resistor R_e. Then, the R_e is determined by

$$R_e = \frac{v_g(t)}{i_g(t)} \quad (6)$$

where $i_g(t)$ is the input current.
Substitute equation (6) to equation (5), therefore, the input current $i_g(t)$ can be yielded from

$$i_g(t) = \frac{V_o}{R_e}(1-d(t)) \quad (7)$$

where the output voltage is the small-ripple approximation so that $v_o(t) \approx V_o$.
Equation (7) is an original equation for realizing the circuit implementation of control system shown in Fig. 2a. However, for creating the original equation for control system in Fig. 2b, equation (8) is applied. Here, the input current is equal to the average value of the switch current so that

$$\frac{1}{T_s}\int_0^{d(t)T_s} i_s(\tau)d\tau = \frac{V_o}{R_e}(1-d(t)) \quad (8)$$

To realize the relation in equation (7) and (8) to implement the proposed control circuits, the relation of the voltage form is required. So, the sensing circuit resistor R_s is defined and added to equation (7) and (8). Then, the new relation for induction current control type in Fig.2a can be yielded as

$$R_s i_g(t) = R_s \frac{V_o}{R_e}(1-d(t)) \quad (9)$$

where R_s is the sensing circuit resistor.
And the relation for switch current control type can be yielded as

$$\frac{R_s}{T_s}\int_0^{d(t)T_s} i_s(\tau)d\tau = R_s\frac{V_o}{R_e}(1-d(t)) \quad (10)$$

or

$$R_s\langle i_s(t)\rangle_{T_s} = R_s\frac{V_o}{R_e}(1-d(t)) \quad (11)$$

where $\langle i_s(t)\rangle_{T_s}$ is the average value of the switch current $i_s(t)$.
To obtain a duty $d(t)$ to satisfy equations (9) and (11), the voltage signal from current sensor is compared with the periodic carrier waveform $v_c(t)$ which is realized by substituting $d(t)$ with t/T_s in equation (9) or (11) so that,

$$R_s i_g(t) = v_c(t) \quad (12)$$

or

$$R_s i_g(t) = V_m\left[1-\frac{t}{T_s}\right] \quad 0 \le t \le T_s \quad (13)$$

where V_m is the control signal from the error amplifier in the voltage feedback loop $A_v(s)$. Then, the negative slope ramp carrier waveform $v_c(t)$ can be obtained by

$$v_c(t) = V_m\left[1-\frac{t}{T_s}\right], \quad 0 \le t \le T_s$$
$$v_c(t+T_s) = v_c(t) \quad (14)$$

By using equations (9) and (13), the emulated resistance R_e can be determined by

$$R_e = R_s\frac{V_o}{V_m} \quad (15)$$

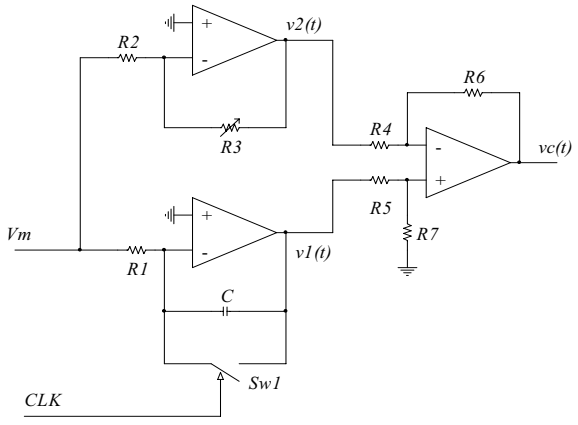

Fig. 4 Implementation of negative slope ramp generator (where *CLK* is the fixed frequency clock signal, Sw_1 is the integrator switch.)

To implement the generator circuit of the negative slope ramp carrier waveform, equation (14) is used. Firstly, the

control signal V_m is integrated by using the well-known inverting integral with reset clock circuit for creating term so that,

$$v_1(t) = -\frac{1}{T_s}\int V_m dt \; ; 0 < \tau < dT_s \qquad (16)$$
$$v_1(t) = -\frac{V_m}{T_s}t$$

where duty $d(t)$ is equal to t/T_s.
And at the same time V_m is amplified by using the inverting amplifier circuit so that

$$v_2(t) = -1 \times V_m = -V_m \qquad (17)$$

and both signals are compared by using the differential amplifier.

$$v_c(t) = \left[v_1(t) - v_2(t)\right] = \left[-\frac{V_m}{T_s}t - (-V_m)\right] \qquad (18)$$
$$v_c(t) = V_m\left[1 - \frac{t}{T_s}\right], \quad 0 \le t \le T_s$$

The circuit implementation of the negative slope ramp waveform generator that realized from equation (14) is shown in Fig.4.

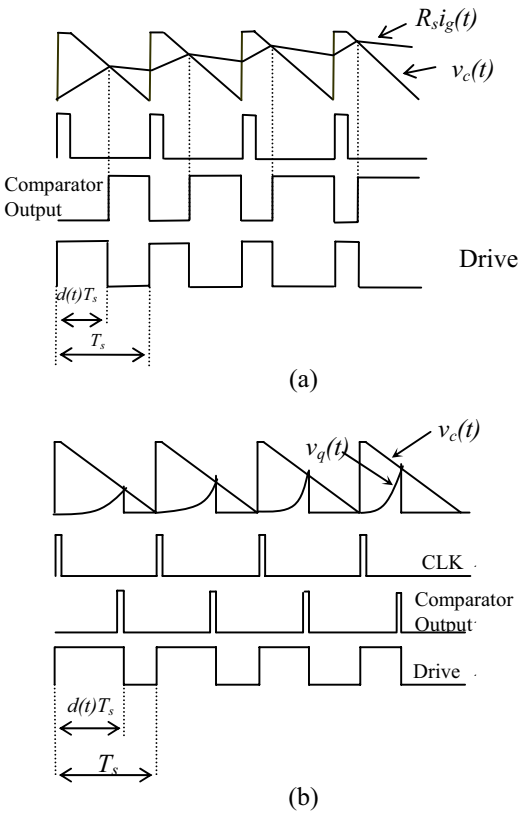

Fig. 5 Control circuit operation of proposed controller: (a) inductor current sensing type and (b) switch current sensing type

Fig.5a shows the operation of control circuit in Fig.2a. Here, the boost converter is sensed and compared to the negative slop ramp waveform at the comparator. At the beginning of a switching period, a short clock pulse sets the flip-flop (*FF*), which turns on the power switch Q. The reset of the *FF* is based on the comparison of the signal from the inductor current sensing circuit $R_s i_g(t)$ and the negative slope ramp carrier waveform $v_c(t)$. At $R_s i_g(t) = v_c(t)$, the comparator output goes high and resets the *FF* turning off the power switch Q as shown in drive signal in the figure (lower trace). The process is repeated in each switching period. For the operation of control circuit in Fig.2b, the switch current is sensed and integrated at integrator circuit. This signal is compared with the negative slope ramp waveform at the comparator. It almost has same procedure with the control system operation in Fig.5a but has some different in signal waveshape as shown in the figure (current signal has parabolic waveshape).

To ensure the proposed control operating in CCM, the determination of CCM and DCM conditions when load is varied must be analyzed. In the analysis, we use the following notations for normalized input voltage $v_g(t)$ and its peak value is $V_{g,peak}$

$$m_g = \frac{v_g(t)}{V_o} \qquad (19)$$

$$M_g = \frac{V_{g,peak}}{V_o} \qquad (20)$$

where $m_g(t)$ is the DC-DC conversion ratio and M_g is the peak value of the $m_g(t)$.
When the boost converter operates in the DCM, the input current can be written as

$$i_g(t) = \frac{1}{2}\frac{v_g(t)}{L_P}d^2(t)T_s \qquad (21)$$

So, the boost converter will operate in the CCM when,

$$\frac{v_g(t)}{R_e} > \frac{1}{2}\frac{v_g(t)}{L_p}d^2(t)T_s \qquad (22)$$

By using the relations in (7), (19), (20) and (22), the relation of the DC-DC conversion ratio and duty ratio can be yielded as

$$\frac{M_g^2}{2}\frac{m_g(t)}{K}d^2(t) + d(t) - 1 = 0 \qquad (23)$$

where R is the DC load resistance $R = V_o/I_o$, and $K = 2Lf_s/R$ is the load parameter commonly used in DCM analysis and the relation $V_{g.rms}^2 / R_e = V_o^2 / R$was used to get $R_e / R = M_g^2 / 2$ (where V_{grms} is the root mean square value of the input voltage vg(t)and f_s is switching frequency).

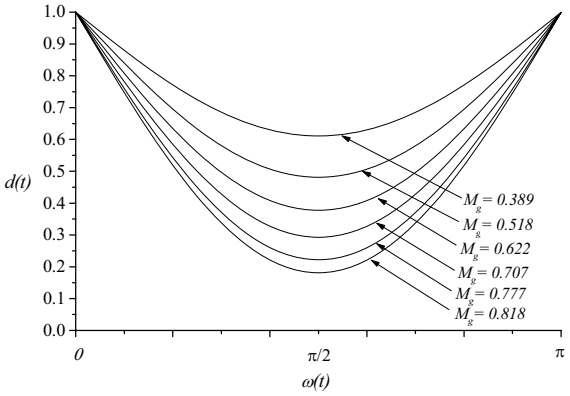

Fig. 6 Plots of duty ratio of the high power factor boost converter with proposed control

To consider the boundary between the CCM and the DCM operations, the relation as shown in (20) is defined.
Use the relation in (19), (20), and (22) substitute in (23), then

$$K > \frac{1}{2} M_g^2 (1 - m_g(t)^2) \tag{24}$$

From (24), we conclude that the boost pre-regulator is always in the CCM if

$$\frac{2Lf_s}{R} = K > \frac{M_g^2}{2} \tag{25}$$

and always operates in the DCM if

$$K < \frac{1}{2} M_g^2 (1 - M_g)^2 \tag{26}$$

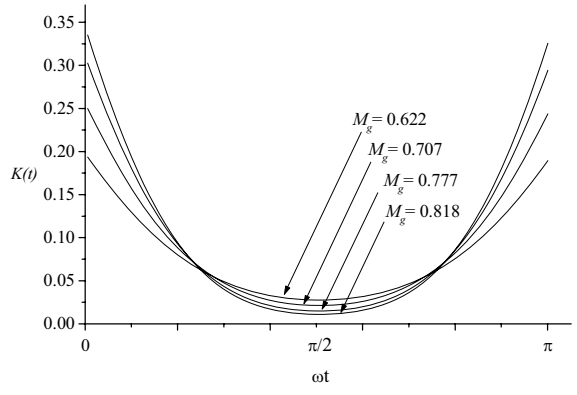

Fig. 7 Plots of load parameters of the proposed control

Relation in (5) is used to make the plots of the duty ratio *d(t)* of the proposed controller for several values of the conversion ratio Mg and these plots are shown in Fig.6.
Relations (24), (25) and (26) are used to make the plots of the load parameters *K(t)* of the proposed control operated by the duty ratio *d(t)* from relation in (23) at several conversion ratio M_g values as shown in Fig.7.

To design the output voltage regulating loop, the small signal ac frequency modeling is necessary. The relation in (11) is used to be considered and can be re-written as

$$R_s i_g(t) = v_m(t)(1 - d(t)) \tag{27}$$

where $v_m(t)$ is the control signal that varies with time at the second harmonic of ac line frequency 2ω.
then,

$$R_s i_g(t) = R_s \frac{v_g(t)}{R_e} \tag{28}$$

So, the relation of input current $i_g(t)$ can be yielded by

$$i_g(t) = \frac{v_m(t)}{R_s} \frac{v_g(t)}{v_o(t)} \tag{29}$$

where the output voltage $v_o(t)$ is varied with time at the second harmonic of AC line frequency 2ω.
Then the output current of the boost converter is

$$\hat{i}_o(t) = \frac{2V_{g,rms}}{V_o^2} \frac{V_m}{R_s} v_{g,rms}(t) - \frac{2V_{g,rms}^2}{V_o^3} \frac{V_m}{R_s} \hat{v}_o(t) + \frac{1}{R_s} \frac{V_{g,rms}^2}{V_o^2} \hat{v}_m(t) \tag{30}$$

Here, we define the notation of the small signal AC frequency modeling of the high power factor boost converter with the proposed control from equation (30) as,

$$\hat{i}_o(t) = g_o v_{g,rms}(t) + g_m \hat{v}_m(t) - \frac{\hat{v}_o(t)}{r_o} \tag{31}$$

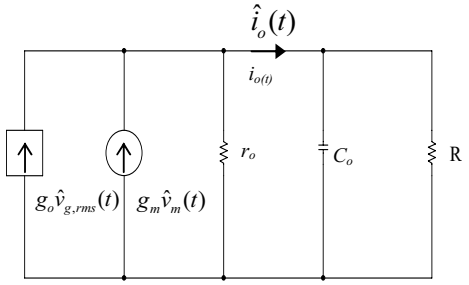

Fig. 8 Small signal ac frequency modeling of the boost pre-regulator with the proposed control method (where C_o = the output capacitor of the boost converter and *R* is the output resistor of the boost converter)

By using the relation in equation (31), the small signal AC frequency modeling circuit for designing the error amplifier of the output voltage regulating loop can be shown in Fig.8.

III. Experimental Verification Results

The negative slop ramp carrier control using switch current sensing was selected to verify the proposed control method for controlling the high power factor boost converter. The circuit experiments were applied by designing to meet the following specifications:

The output power P_o = 350 W, the output voltage V_o = 440 V_{dc}, the input voltage $V_{g,rms}$ = 220 V_{rms}, the line frequency f = 50 Hz, the switching frequency f_s = 40 kHz, Inductance (L) = 2.5 mH, and the load resistance R at full load is equal to 500 Ω.

From the small signal AC frequency modeling in Fig.7, the transfer function $F(s)$ of the high power factor boost converter with the proposed control method can be yielded as

$$F(s) = \frac{\hat{v}_o}{\hat{v}_m} = \frac{g_o}{3} R \frac{1}{(1 + \frac{s}{\omega_p})} \tag{32}$$

Here, the converter pole frequency is defined as $\omega_p = 3/RC_o$ Therefore, the voltage regulating control loop gain $T(s)$ can be determined from

$$T(s) = A_v(s)F(s)H(s) \tag{33}$$

We define the transfer function of the error amplifier of the voltage control mode $A_v(s)$ as

$$A_v(s) = \frac{\left(1 + \frac{s}{\omega_{z1}}\right)}{\left(\frac{s}{\omega_o}\right)\left(1 + \frac{s}{\omega_{z2}}\right)} \tag{34}$$

where ω_o is the amplifier frequency, ω_{z1} is the compensator zero frequency No.1, and ω_{z2} is the compensator zero frequency No.2. Then, equation (33) can be re-written as

$$T(s) = \frac{g_o}{3} R \frac{1}{(1 + \frac{s}{\omega_p})} \frac{\left(1 + \frac{s}{\omega_{z1}}\right)}{\left(\frac{s}{\omega_o}\right)\left(1 + \frac{s}{\omega_{z2}}\right)} H(s) \tag{35}$$

where $H(s)$ is the output voltage sensor gain.
Equation (35) is used to implement the output voltage regulator, which has the circuit parameters as shown in the experimental circuit in Fig.9.

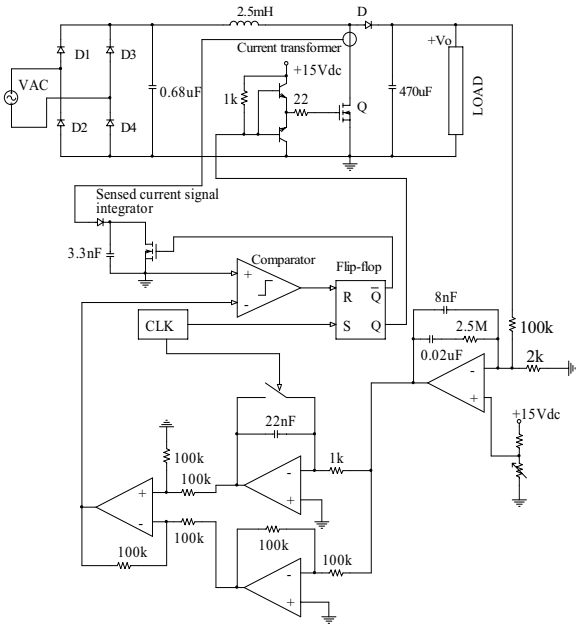

Fig. 9 Experimental circuit of 350 W high power factor boost converter with proposed control for switch current sensing type

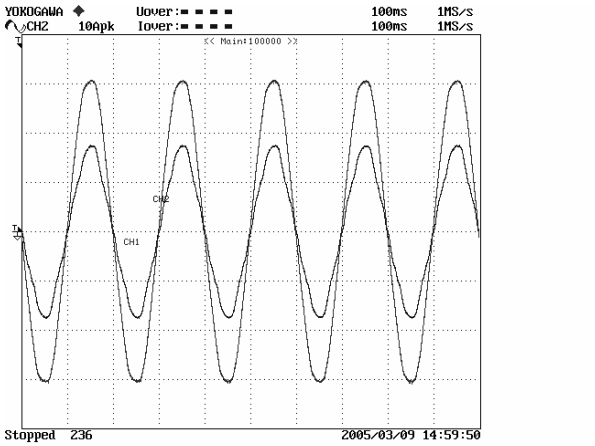

Fig. 10 Experimental waveforms at full load condition (topper) input voltage [CH1:100 V/Div, 1 ms/Div], and (lower) input current [CH2:2 A/Div, 1 ms/Div]

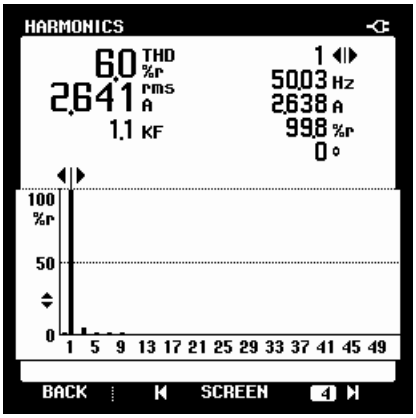

Fig. 11 Spectrum of input current waveform at full load condition

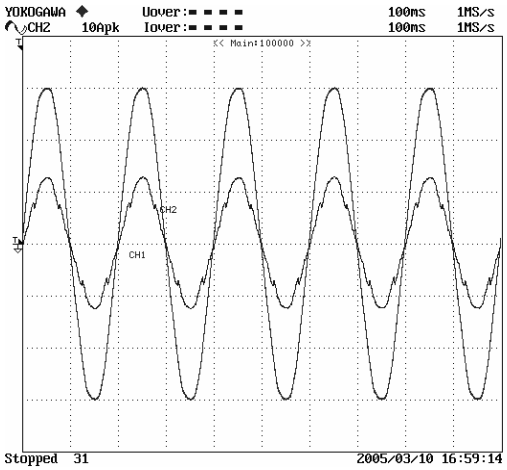

Fig. 12 Experimental waveforms at half load condition (topper) input voltage [CH1:100 V/Div, 1 ms/Div], and (lower) input current [CH2:2 A/Div, 1 ms/Div]

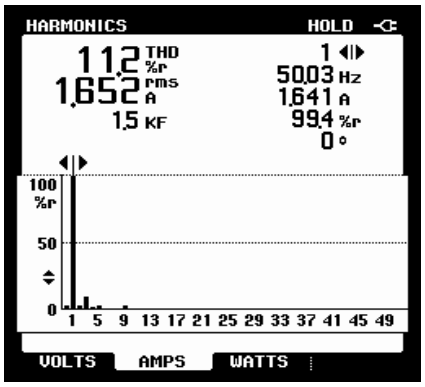

Fig. 13 Spectrum of input current waveform at half load condition

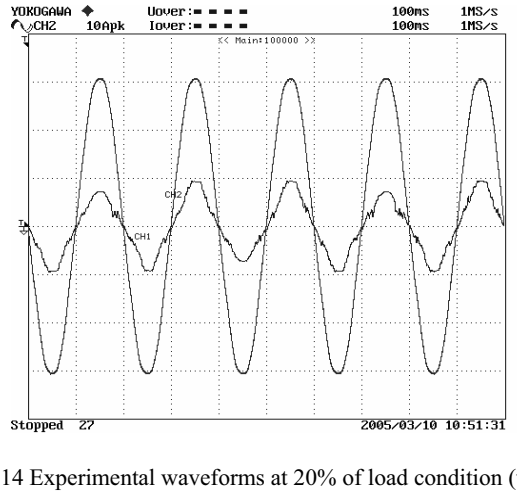

Fig. 14 Experimental waveforms at 20% of load condition (topper) input voltage [CH1:100 V/Div, 1 ms/Div], and (lower) input current [CH2:2 A/Div, 1 ms/Div]

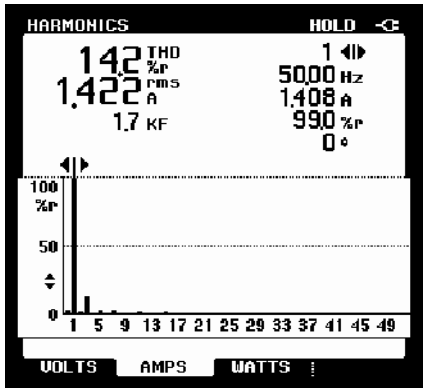

Fig. 15 Spectrum of input current waveform at 20% of load condition

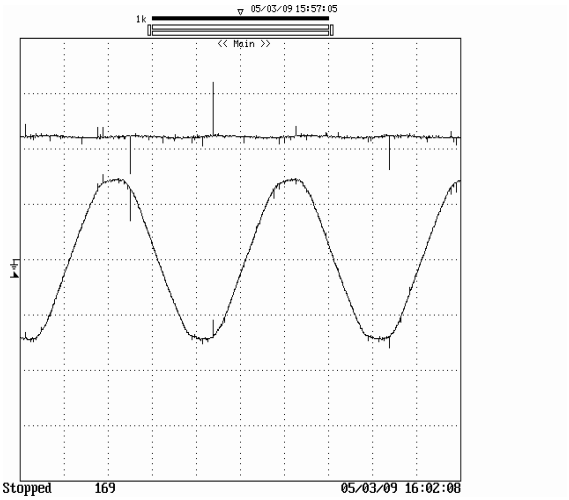

Fig. 16 Experimental waveforms at full load condition (topper) output voltage [CH1:200 V/Div, 5 ms/Div], and (lower) input voltage [CH2:200 V/Div, 5 ms/Div]

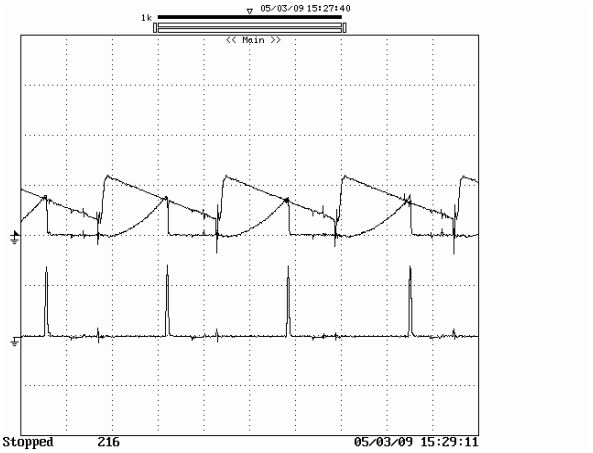

Fig. 17 Experimental waveforms of control circuit operations (topper) negative slope ramp carrier waveform [CH1: 15V/Div, 10μs/Div], (middle) integrating signal from switch current sensing circuit [CH2:15V/Div, 10μs/Div], and (lower) clock signal [CH3:15V/Div, 10μs/Div].

By using the proposed control method controlling the operation of the high power factor boost converter, the input current waveform (shown in Fig.10 lower trace) was shaped to be closely sinusoidal by following the input voltage waveform that having %THD in current as 6% (shown in Fig.10 topper trace). Fig.11 shows the spectrum of input current waveform at full load condition, which shown in Fig.10. Although half load condition or lower was yielded to the high power factor boost converter, the input current waveform was still closely sinusoidal as shown in Fig.12 and 14 (lower trace) and theirs spectrum were shown in Fig.13 and 15. In the figures, the total harmonic distortion (%THD) was not exceeded 15%. Fig.16 shows while the input current was shaped to be closely sinusoidal, the output voltage was regulated to specified value (440V). The control circuit operation waveforms were shown in Fig.17.

IV. Conclusion

The high power factor boost converter using proposed control method in CCM operation was introduced and verified by the experiment of 350W boost converter. The proposed control method requires only the output voltage and inductor current sensors. So, the error amplifier in the current control mode, the input voltage sensor, and the multiplier used in the conventional controller are not required. The duty ratio is determined by comparing the integral of sensed switch current with the negative slope ramp carrier waveform in each switching period. By using the proposed control method, the input current waveform of boost converter was shaped to be closely sinusoidal by following the input voltage waveform.

References

[1] D. Chambers and D. Wang, Dynamic P.F. correction in capacitor input off-line converters, in Proc. Powercon 6, Miami Beach, FL, May 2-4, 1979, pp, B3.1-6.

[2] M. Kazerani, P.D.Ziogas and G.Joos, "A novel active current waveshaping technique for solid-state input power factor conditioners," *IEEE Trans. Industry Electronics*, vol.38, no.1, February 1991.

[3] D.Maksimovic, Design of the Clamped-Current High-Power-Factor Boost Rectifier, APEC Conf. Proc., 1994, pp.584-590.

[4] D. Maksimovic, Yungtaek Jang, and Robert W. Erickson, Nonlinear-Carrier Control for High Power Factor Boost Rectifiers, IEEE Trans. Power Electronics, vol. 11, No. 4, March 1996, pp. 578-584.

[5] R. Zane and D. Maksimovic, Nonlinear-Carrier Control for High Power Factor Based on Up-Down Switching Converters, in IEEE Trans. Power Electronics, vol. 13, No. 2, March 1998, pp. 213-221.

[6] J. P Gegner, C. Q. Lee, Linear Peak Current Mode Control: A Simple Active Power Factor Correction Control Technique for Continuous Conduction Mode, PESC Conf.Proc., 1996, pp. 196-202.

[7] J. R. Rajagopalan, P. Nara, F. C. Lee, A generalized Technique for Derivation of Average Current Mode Control Laws for Power Factor Correction without Input Voltage sensing, APEC Conf. Proc., 1997, pp. 81-87.

[8] J. Hwang, A. Chee and W. H. Ki, New Universal Control Methods for Power factor Correction and DC to DC Converter Application, Applied Power Electronics Conference and Exposition, 1997. APEC '97 Conference Proceedings 1997, Twelfth Annual, Volume: 1, 1997 Page(s): 59 -65 vol.1.

[9] Z. Lai and K. Smedley, A General PWM Modulator and Its Applications , IEEE Transactions on Circuits and Systems I: Fundamental Theory and Applications, April 1998, vol.45, (no.4):386-96.

[10] T. Tanitteerapan, and S. Mori, Fundamental frequency Parabolic PWM Controller for Lossless Soft-switching Boost Power Factor Correction, IEEE International Symposium on Circuits and Systems, 2001. ISCAS'01, May, Sydney Australia, Vol.3, pp. 57-60.

[11] T. Tanitteerapan, and S. Mori, A Simple Continuous Conduction Mode PWM Controller for Boost Power Factor Correction Converter, IEEE The 2002 International Technical Conference on Circuits/Systems, Computers and Communications, 2002. ITC-CSCC 2002, July 16-19, Phuket, Thailand.

[12] T. Tanitteerapan, Averaging Switch Current Controller for High Power Factor Boost AC-DC Pre-Regulators, The 3rd International Symposium on Communications and Information Technologies, 2003. ISCIT 2003, September 3-5, Songkhla, Thailand, pp. 315-318.

[13] T.Tanitteerapan, and E.Thanpo, Low harmonic currents pre-regulator based on DC-DC boost converters for switching power supply in instrumentation system, International Conference on Instrumentation, Control and Information Technology (SICE 2005), August 8-10, Okayama University, Okayama, Japan.

T. Tanitteerapan was born in Yala, Thailand, in 1971. He received the B.S.Ind Ed. in electrical engineering in 1994 from King Mongkut's University of Technology Thonburi, Bangkok, Thailand, the M.S degree in High Voltage Measuring System from Department of Electrical and Electronics Engineering, Nippon Institute of Technology, Saitama, Japan in 2000 and the Doctor of Engineering in Power Electronics Engineering at Mori Shinsaku Laboratory, Nippon Institute of Technology, Japan in 2003. Currently he is Assistant Professor of Department Electrical Technology Education, Faculty of Industrial Education, King Mongkut's University of Technology Thonburi, Thailand. His research interests include soft-switching power factor correction converters, simple wave shaping techniques for high power factor rectifiers in CCM operation, single-stage power factor correction converters, Photovoltaic Powered Applications, Electrical Teaching Methods.

Ekkachai Thanpo was born in Nakorn Sri Thammarat, Thailand, in 1975. He received the B.S.Ind Ed. in electrical engineering in 1998 from Nakorn Sri Thammarat Technical Collage, Nakorn Sri Thammarat, Thailand, the M.S degree in Power Electronics from Department of Electrical Technology Education, King Mongkut's University of Technology Thonburi, Thailand, in 2004. His research interests include soft-switching power factor correction converters, simple wave shaping techniques for high power factor rectifiers in CCM operation, single-stage power factor correction converters, Photovoltaic Powered Applications, Electrical Teaching Methods.